General Disclaimer

One or more of the Following Statements may affect this Document

- This document has been reproduced from the best copy furnished by the organizational source. It is being released in the interest of making available as much information as possible.

- This document may contain data, which exceeds the sheet parameters. It was furnished in this condition by the organizational source and is the best copy available.

- This document may contain tone-on-tone or color graphs, charts and/or pictures, which have been reproduced in black and white.

- This document is paginated as submitted by the original source.

- Portions of this document are not fully legible due to the historical nature of some of the material. However, it is the best reproduction available from the original submission.

Produced by the NASA Center for Aerospace Information (CASI)

(NASA-CR-162170) RESEARCH ON RADIATION INDUCED LASER PLASMAS Semiannual Report (Florida Univ.) 43 p HC A03/MF A01 CSCL 20I

N79-32097

Unclas

G3/75 31967

SEP 1979
RECEIVED
NASA STI FACILITY
ACCESS DEPT.

ENGINEERING AND INDUSTRIAL EXPERIMENT STATION

College of Engineering

University of Florida

Gainesville

SEMIANNUAL REPORT

RESEARCH ON RADIATION INDUCED LASER PLASMAS

by

Richard T. Schneider, Michael J. Rowe
B. Dudley Carter, Roy A. Walters, John
D. Cox, Roger Liang, Tim Roxey and
Luis Zapata

NASA GRANT
NSG 1586

Department of Nuclear Engineering Sciences
University of Florida
Gainesville, Florida

September, 1979

TABLE OF CONTENTS

	Page No.
INTRODUCTION	1
NUCLEAR PUMPED CW-CO_2 LASER	2
1. Background	2
2. Results	7
SPECTRAL EMISSION OF NUCLEAR EXCITED NOBEL GASES	10
1. Background	10
2. Results	10
OPTICAL COMPATIBILITY OF UF_6 WITH LASER GASES	16
1. Background	16
2. Results	20
APPENDIX	26
NUCLEAR PUMPED CW-LASING OF THE He^3-Ne SYSTEM by B. D. Carter, M. J. Rowe and R. T. Schneider (Article submitted to Applied Physics Letters)	

INTRODUCTION

The program at the University of Florida is concerned with contributing to the development of high power nuclear pumped lasers.

In order to justify the use of a nuclear reactor as an energy source for a laser system, the laser power extracted has to constitute an appreciable part of the reactor power. For this reason, demonstration of feasibility of high powered nuclear-pumped lasers should have the highest priority. It is suggested that high-energy output can be achieved easier by CW operation than by single pulse. This reasoning defines the direction of the research as follows:

1. Work on CW-He-Ne nuclear-pumped laser, the motivation being a better understanding of the excitation mechanism.
2. Work on a CO_2-nuclear-pumped laser, the motivation being to demonstrate CW output in the order of watts.
3. Identify laser gases which are compatible with UF_6 by excited states lifetime measurements, the motivation being the assumption that high-power densities are only achievable by volume fission fragment sources.
4. Examine Xe_2, XeF and KrF under nuclear irradiation to determine if they are good candidates for nuclear-pumped lasers.

NUCLEAR PUMPED CW-CO_2-LASER

1. Background

A nuclear pumped CO_2 laser has not been demonstrated so far. However, nuclear augmentation of an electrically excited laser was demonstrated a few years back. In this case, input of nuclear energy into the laser was small compared to the electrical input. In the present work an attempt was made to reverse this situation. This is based on the fact that in the previous experiment, a neutron flux of only 10^{10} neutrons/sec cm^2 was available to provide the nuclear power input, which amounted to a few milliwatts (Figure 1). In the present experimental set-up a neutron flux of 10^{14} n/cm^2 is available, which provides a nuclear power input of up to 100 watts to the laser when operating at a peak power (5 megawatts thermal). The reactor also has the advantage of providing a port large enough (6 inch diameter) to allow insertion of the laser (Figure 2). The laser system consisted of five parts:

1. The laser was an 85 cm pyrex water cooled tube with a 16 mm bore. The windows were NaCl mounted at the proper Brewester angle. The cavity was a 1 meter long aluminum tube with a 10 meter radius hole-coupled mirror at one end and one flat mirror on the other. Both mirrors were gold coated pyrex. (Figure 3).

2. The laser was mounted into a canister-beam plug. This is a secondary containment as well as a radiation shield. Both of these parts are necessary to meet safety requirements. (Figure 4).

3. Power supplies: the power supply was provided, 50 KV, 200ma DC. Available instrumentation consisted of current and voltage meters as well as a plotter set up for I-V curves.

4. Gas System: The vacuum station is capable of 10^{-7} torr to insure the purity of the laser gas. Total pressure was monitored by a thermocouple gauge, a Wallace and Turner gauge and a capacitance manometer.

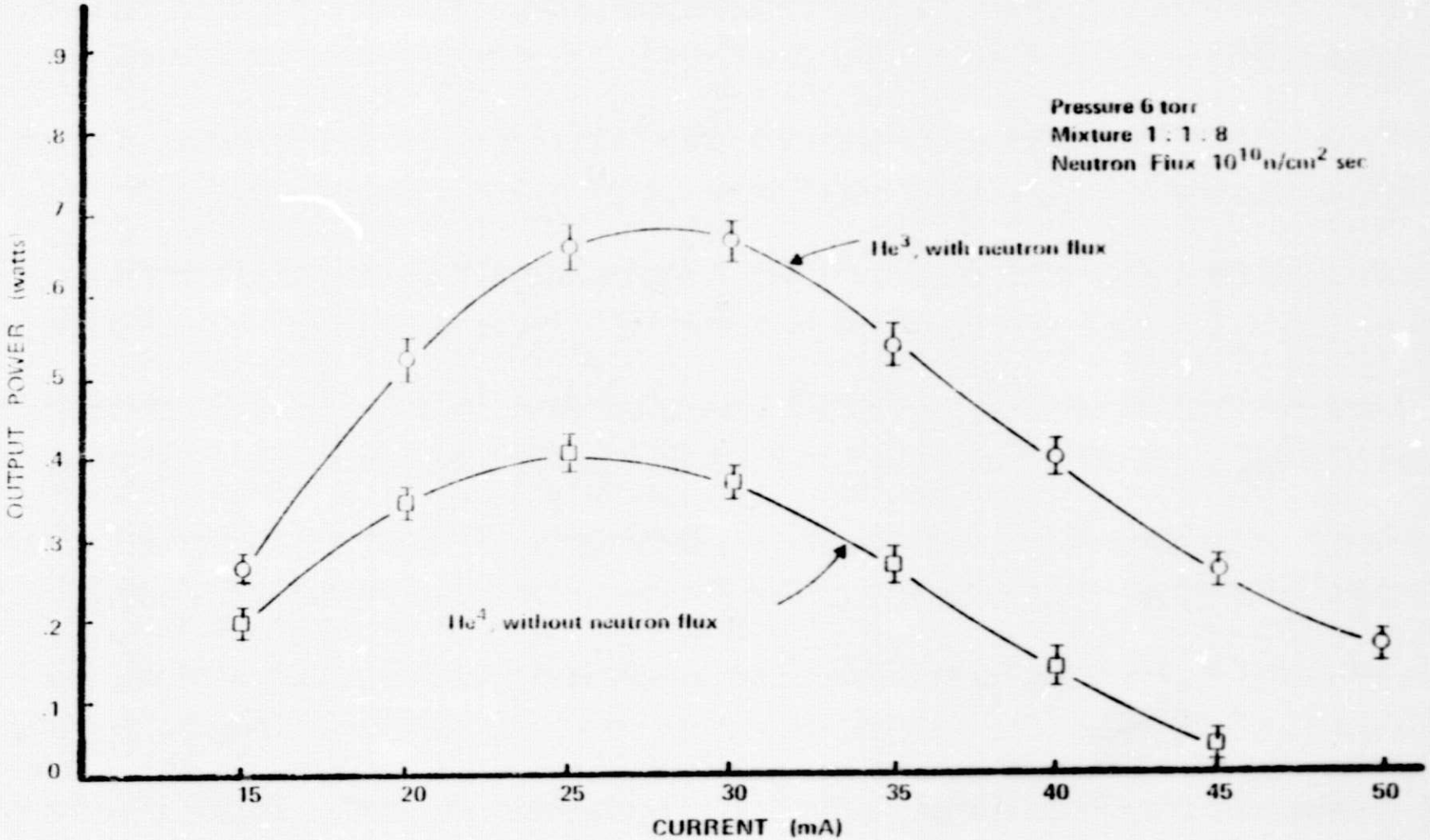

FIG. 1. LASER POWER ENHANCEMENT WITH NEUTRON IRRADIATION

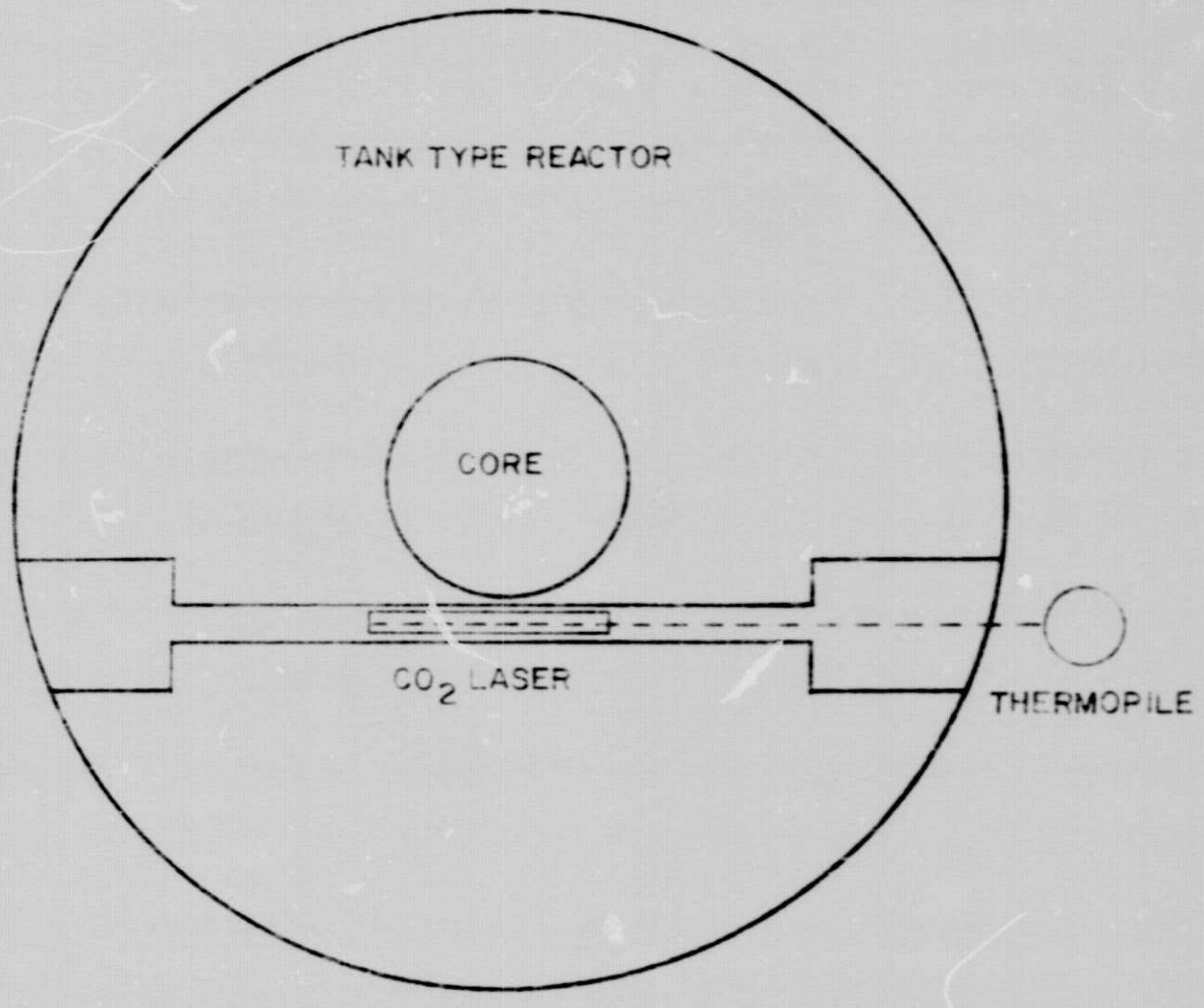

FIG. 2. Location of Experiment in the Nuclear Reactor

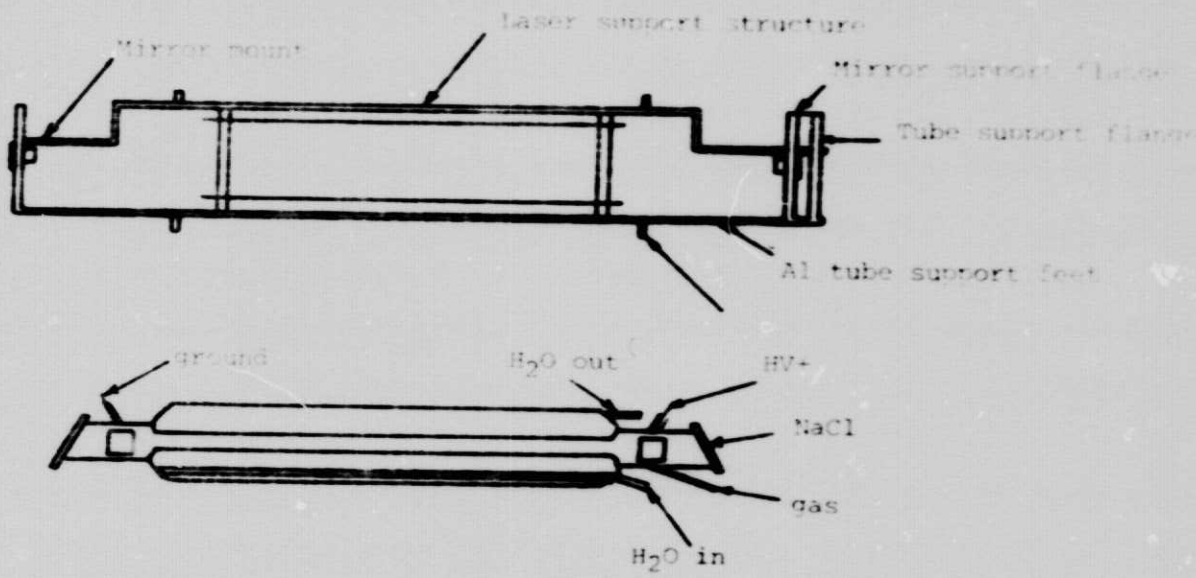

FIG. 3. CO_2 Nuclear Laser System

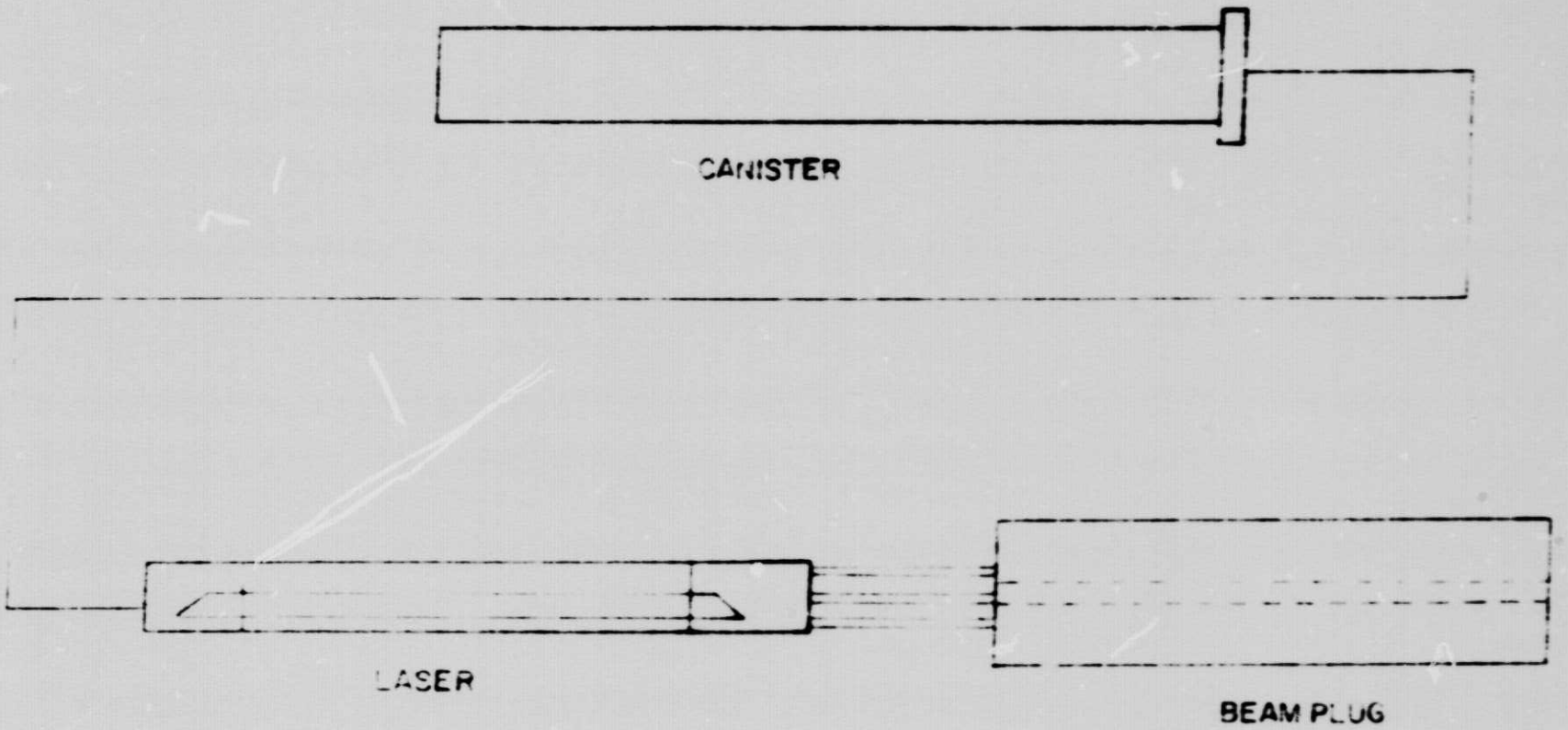

FIG. 4. CANISTER-BEAM PLUG ASSEMBLY

5. Beam Monitor: a thermopile was used to determine laser output, which was recorded by a strip chart recorder. To determine observed laser transition, a CO_2 spectrum analyzer was used.

2. Results

Three runs at three pressure of CO_2 were made. The gas used consisted of a premix of 1:1:8 CO_2:N_2:He^4 at a total pressure of 10 torr. After verification of laser action, the proper amount of He^3 was added to bring the total pressures up to 20, 60 and 300 torr. Each time a breakdown voltage of 13 KV-DC was applied across the laser tube. When breakdown occurred, the current was maintained at 25ma by changing the voltage as necessary.

During the first run at 20 torr total pressure (see Figure 5), the laser would operate with the reactor at zero power. At a reactor power of about 10 KW or 10^{11} n/cm^2-sec, laser power output increased 25% with no change in current or voltage.

During the second run of 60 torr total pressure, the laser would not break down at zero reactor power. The discharge did start at a reactor power of about 10KW or 10^{11}n/cm^{2}sec. The power output was lower than that of the 20 torr run but in this case, the laser would only run while subjected to nuclear irradiation.

The third run was at a total pressure of 300 torr. As in the second case, the laser would not break down at zero power. Even at power up to 5000 KW or 10^{14}n/cm^2-sec there was no electrical breakdown, however, at a flux of 2×10^{11}n/cm^2-sec a low power output was seen on the order of 50 mw and less. The lasing action would stop, however, if voltage across the tube was removed. It should be noted though that the current metering devices used will not read any value lower than .5ma. Based on this, there may have been sufficient preonization to account for the laser power.

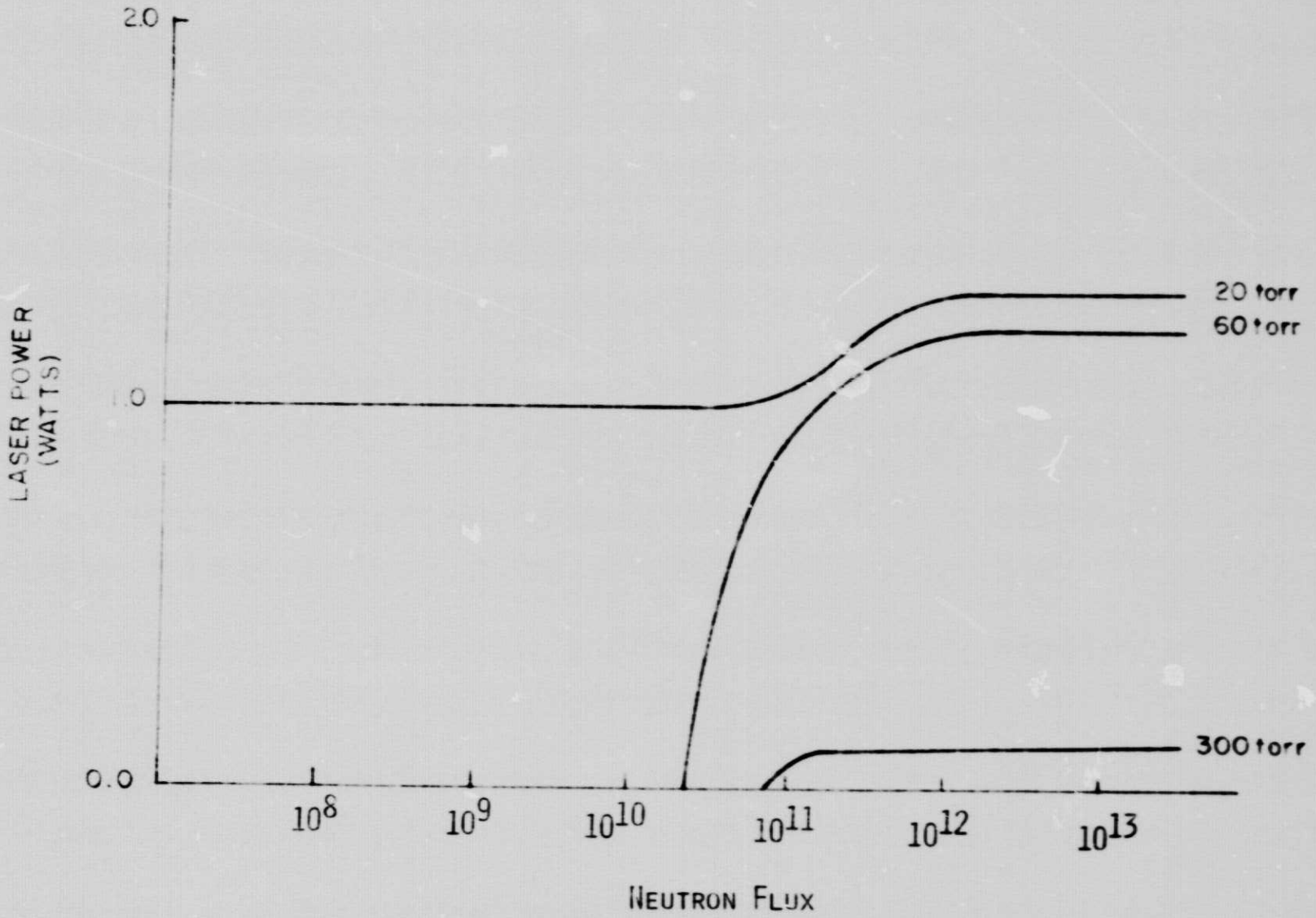

FIG. 5. Output of CW-CO_2 Laser vs. Neutron Flux

Even though there was not a strictly nuclear sustained output at the pressure runs of 60 and 300 torr, it is of significance that the laser would run only under nuclear irradiation.

Even though there was not a strictly nuclear sustained output at the pressure runs of 60 and 300 torr, it is of significance that the laser would run only under nuclear irradiation.

SPECTRAL EMISSION OF NUCLEAR EXCITED NOBLE GASES

1. Background

In order to determine the efficiency of energy transfer from the $^3He(n,p)T$ nuclear reaction to UV and VUV radiation a vacuum-ultraviolet spectroscopy system was employed. The test section consisted of a stainless steel capsule with sapphire windows located in the horizontal throughport of the University of Florida Training Reactor. The radiation investigated was the 172.0 nm band of Xe_2^*, the 355.0 nm band of KrF^* and the 282.0 nm band of $XeBr^*$. Absolute optical calibration was performed using a tungsten ribbon lamp whose emission was determined by both comparison to a NBS calibrated tungsten ribbon source and a calibrated radiometer. This calibration was coupled to a relative calibration (165 to 400 nm) performed internal to the [illegible] system using a standard Deuterium lamp. Spectral scans provided very large easily observed bands for all species studied even though the optical path geometry included only a flat VUV mirror and no elements for focusing on to the monochromator entrance slit. (Figure 6)

2. Result

Using the system described above, radiation of each of the four molecules mentioned above were examined. The energy transfer efficiency from the $He^3(n,p)T$ nuclear radiation to UV-light output was derived from the measurement. A Typical spectrum is shown in Figure 7. Xe-^{3}He mixtures forming Xe_2 were measured to be up to 68 percent efficient. Neither XeF, KrF, nor XeBr had efficiencies greater than 1 percent. These results are summarized in Table 1.

To investigate feasibility of nuclear pumping, UF_6 was added serving at the same time as the florine doner to XeF and KrF. As the concentration of UF_6 is increased, the efficiency of XeF is greatly reduced. In KrF, a concentration of 10% UF_6 will completely quench the line radiation. (See Table 2)

EXPERIMENT FACILITY DESCRIPTION

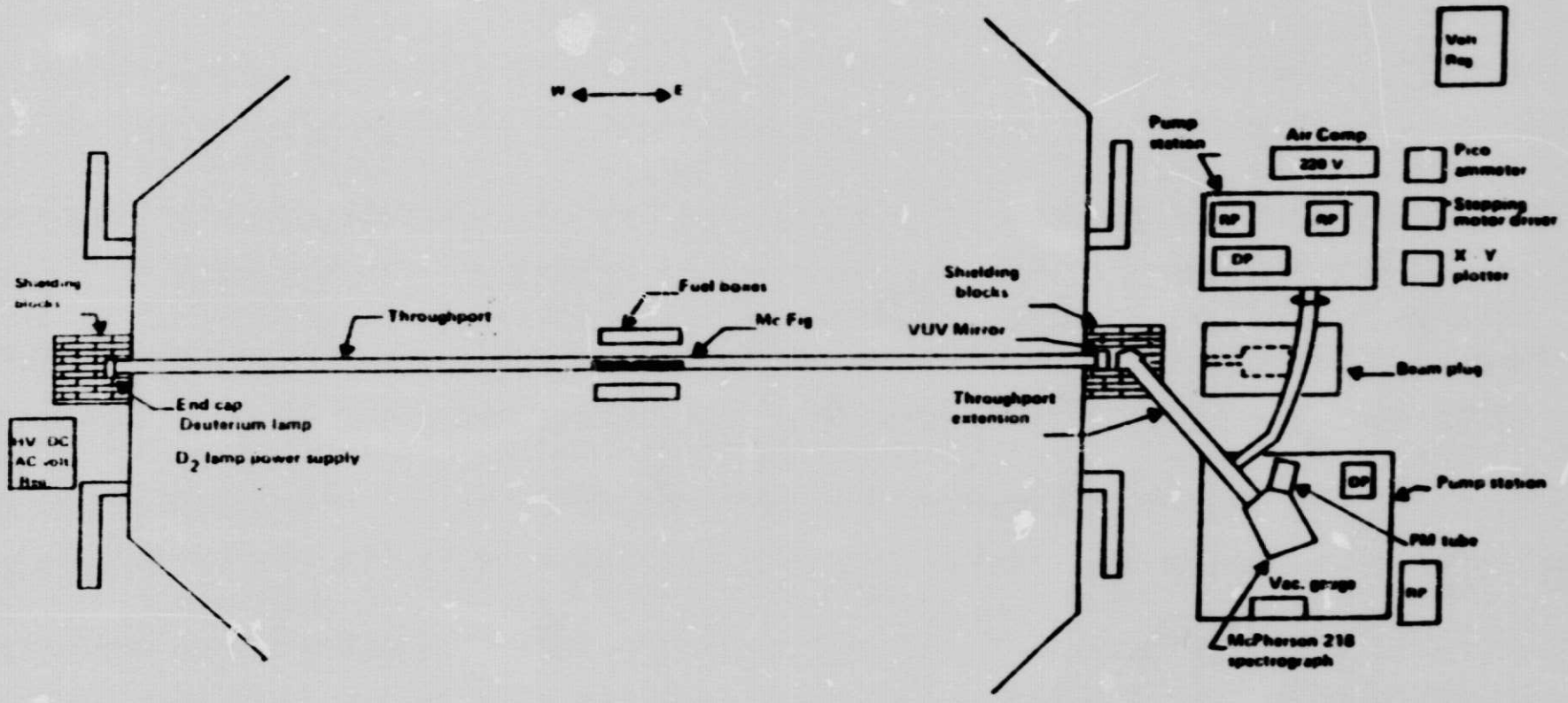

Figure 6. Research facility for vacuum-ultraviolet spectroscopy

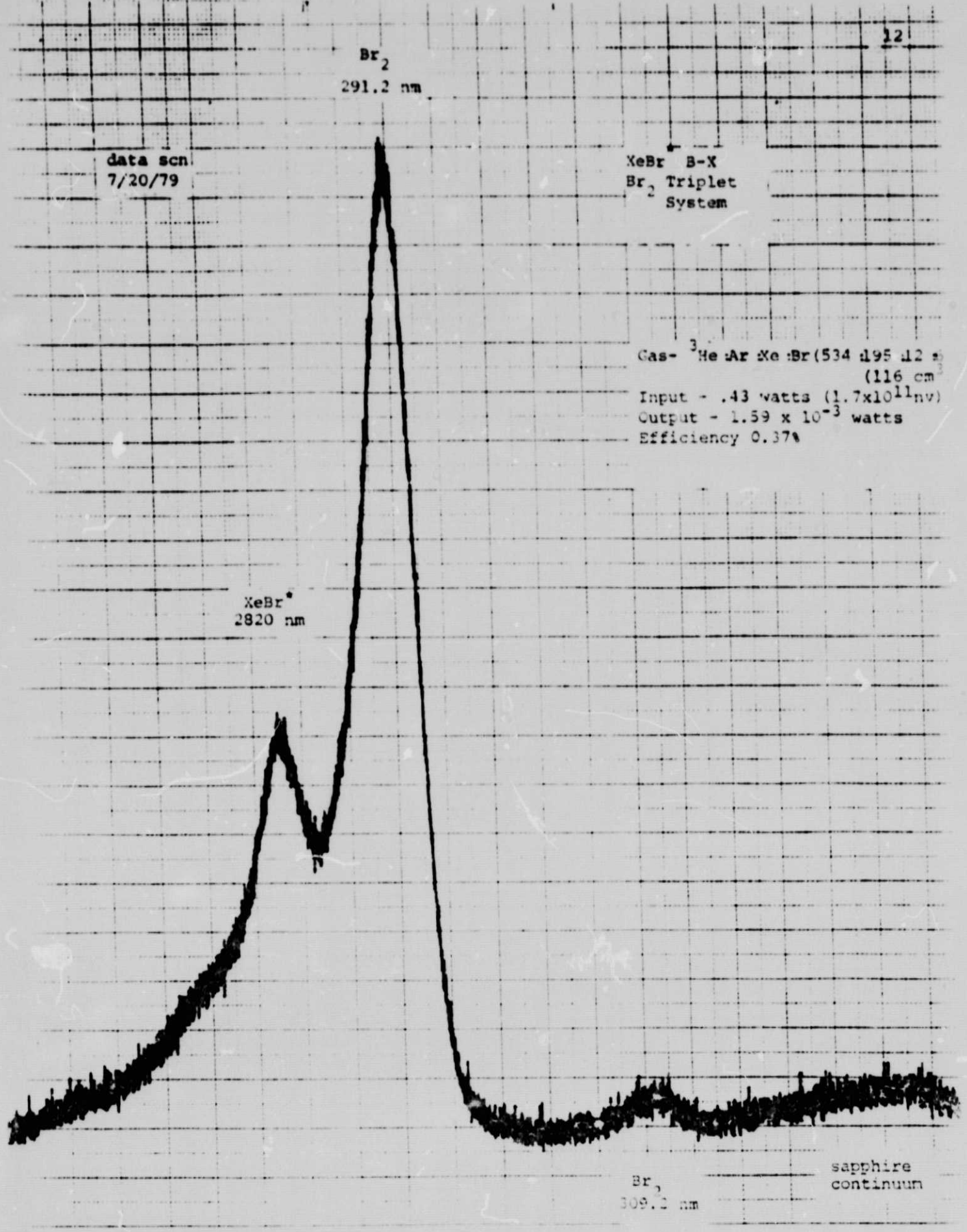

Figure 7 - $XeBr^*$ and Br_2 Emission Bands

REPRODUCIBILITY OF THE
ORIGINAL PAGE IS POOR

REPRODUCIBILITY OF THE ORIGINAL PAGE IS POOR

Table 1. Energy Transfer

Gas	Fill Pressures torr	λ max nm	FWHM nm	Integrated Power Out watts	Input Power watts	Efficiency %	Small Signal gain/meter
XeF*	^{3}He - 507 Xe - 233	172.2	14.9	0.218	0.32	68	1.5×10^{-8}
	^{3}He - 507 Xe - 233	172.2	14.9	0.126	.192	66	
XeF*	^{3}He - 660 Xe - 70 NF_3 - 7	355.0	7.5	6.3×10^{-4}	0.39	0.14	9.61×10^{-9} (2)
	^{3}He - 660 Xe - 66 NF_3 - 6.6	355.0	7.5	6.3×10^{-4}	0.39	0.14	
	^{3}He - 660 Xe - 66 NF_3 - 6.6	355.0	7.5	3.5×10^{-4}	0.39	0.10 (1)	
KrF*	^{3}He - 600 Kr - 100 NF_3 - 7	245.0	5.2	8.2×10^{-4}	0.35	0.23	1.9×10^{-9} (2)

(1) Suspected air contamination.
(2) Effective excited state lifetime not defined for CW case.

REPRODUCIBILITY OF THE
ORIGINAL PAGE IS POOR

Table 2. UF_6 Effects

Gas	Fill Pressures torr	max nm	FWHm nm	Integrated Power Out watts	Input Power watts	Efficiency %	Partial Pressure UF_6-torr	Attenuation % of maximum
XeF*	^3He - 660 Xe - 70 NF_3 - 7	355.0	7.5	6.3×10^{-4}	.39	.14	0	100
(43)	^3He - 600 Xe - 70 NF_3 - 7 UF_6 - 1.6	355.0	7.5	1.95×10^{-4}	.34	.057	1.6	41 (1)
(49)	^3He - 600 Xe - 66 NF_3 - 6.6 UF_6 - 3.2	355.0	7.5	4.35×10^{-5}	.176	.0245	3.2	18 (1)
KrF*	^3He - 568 Xe - 82 UF_6 - 80	--	--	--	.39	0	80	0

(1) A large increase in N_2^+ Bands noted.

The results of this study seem to indicate that there is an excellent coupling between ^3He and Xe_2. However, the coupling between ^3He and XeBr is poor with efficiencies of less than one percent. Also, the results seem to show that UF_6 is a poor substitute as a florine doner since UF_6 is incompatible with the gases investigated even at a reasonable concentration.

The results of this study seem to indicate that there is an excellent coupling between ^3He and Xe_2. However, the coupling between ^3He and XeBr is poor with efficiencies of less than one percent. Also, the results seem to show that UF_6 is a poor substitute as a florine doner since UF_6 is incompatible with the gases investigated even at a reasonable concentration.

OPTICAL COMPATIBILITY OF UF_6 WITH LASER GASES

1. Background

For volume sources for nuclear-pumped lasers, UF_6 is the only practical option for gaseous nuclear fuel. UF_6 will deposit ~260 times more energy into a laser gas than He^3 per neutron interaction. It is imperative to determine the compatibility of UF_6 gas with other laser gases. Not only must they be compatible in the conventional chemical sense, but also in an extended one, namely, that any collision occurring between the gases will not destroy the required population inversion.

One way to investigate optical compatibility is to measure the life-times of excited states including vibrational and electronic deexcitation as well as collisional transfer and recombination effects.

To make these measurements a single photon coincidence counting system has been constructed. By addition of UF_6 to laser gases, their potential for nuclear pumping can be evaluated.

The system can be operated in two different modes. First the pumping of laser gases with fission fragments coming from a Cf^{252} source to determine if the energy deposition from fission events will result in a population of certain states. The second mode is to add natural UF_6 and determine if the gas of interest is still excited into the same states and if the life-time of these states was shortened. Note, it has been demonstrated that 3% UF_6 in a 1:1:8 Co_2:N_2:He laser will still support a population inversion (Figure 8).

The most commonly used non-reactor source of fission fragments for experimental purposes is the radioisotope ^{252}Cf, which spontaneously fissions with a half life of approximately 85 years. (^{252}Cf also decays by α-particle

REPRODUCIBILITY OF THE
ORIGINAL PAGE IS POOR

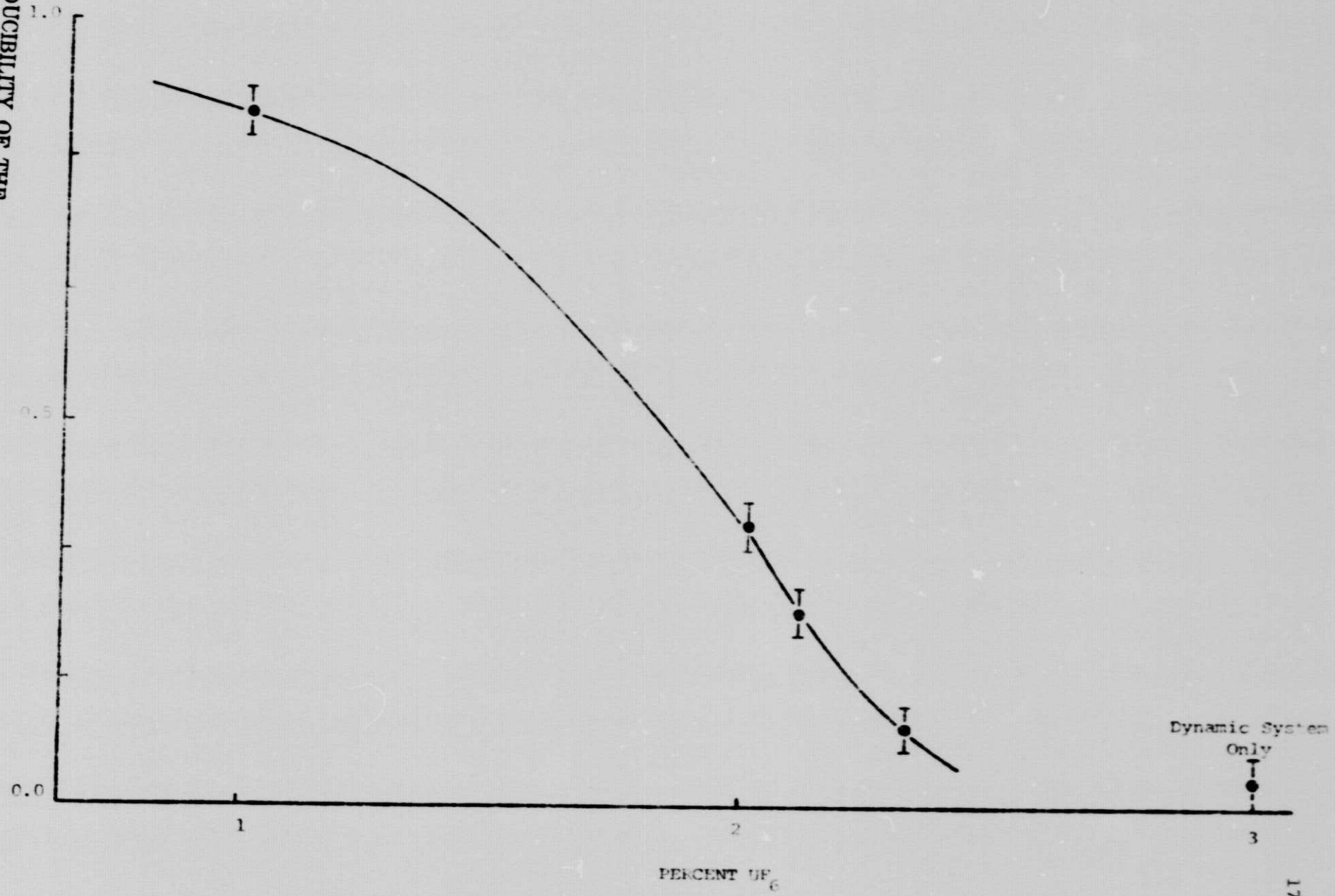

Figure 8. Addition of UF_6 into CO_2 Laser.

emission, yielding an overall half life for its decay of approximately 2.6 years.)

A delayed coincidence single photon counting system has been developed for the study of the excitation of various gases by fission fragments. Figure 9 is a schematic diagram of this system. The light pulse caused by a single fission fragment passing through the gas is viewed by a photomultiplier (PM_1). The output of this photomultiplier passes through a fast crossover discriminator within the base of the PM. This discriminator is set high enough to exclude pulses from the alpha particles and gammas also emitted by the source. The output of this discriminator is a fast logic pulse/related in time to the start of a fission fragment track which triggers the "start" of a time-to-pulse-height converter (TPH). Starting the TPH converter opens a time window of selectable length during which the system can respond to a signal from the monochromator. The photomultiplier on the monochromator is operated in the single photon counting mode and produces a fast pulse for the TPH. The output of the TPH is a pulse, the amplitude of which is proportional to the time between the start and stop pulses.

The system can be operated in several modes, one of which is to set the manochromator on a spectrum line of interest using an internal electrode to electrically excite the gas. The system is allowed to count long enough to build up sufficient statistical accuracy.

The resulting output is a plot of population of the excited state as a function of time. An initial peak is caused by the gammas which come off within 10^{-11} seconds of the fission and provide "zero time." Gammas pass through the body of the PM tube and generate this initial pulse. The rising portion of the curve is the excitation region during which the fission fragment is passing through the gas and causing excitation and ionization. The peak is followed by an afterglow decay period during which the populations of

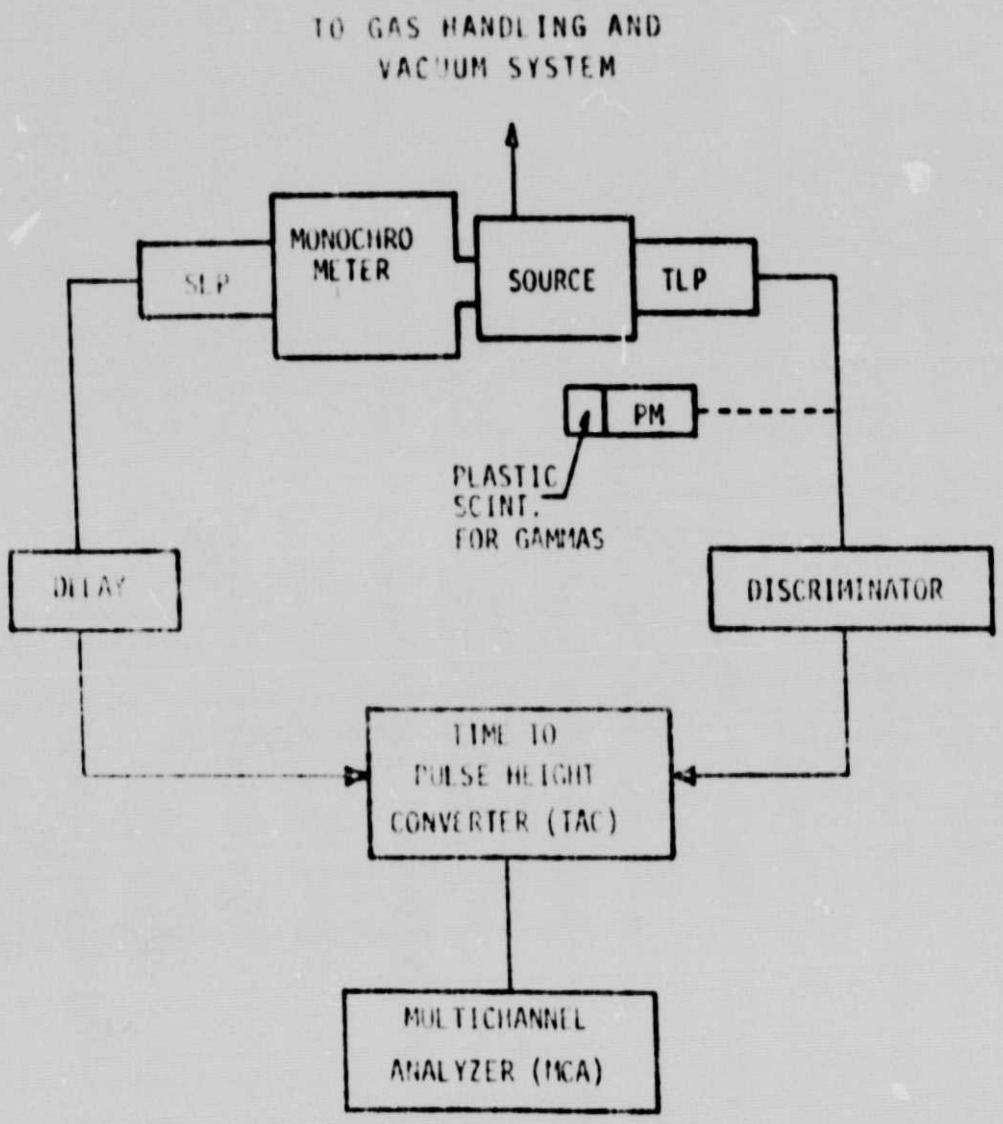

Figure 9. System for Lifetime Measurement

REPRODUCIBILITY OF THE
ORIGINAL PAGE IS POOR

the excited states decay back to zero. From the decay portion of the curve, it is possible to determine

1. lifetimes of excited states,
2. cross-sections for vibrational and electronic deexcitation,
3. collisional transfer cross-sections,
4. electron-ion recombination coefficients, and
5. any other quantity that is usually measured in time resolved intensity measurements.

These quantities can be measured for either fission fragment or alpha particles. The resolving time of the system at present is about 1.5 nanoseconds.

2. Results

The above described technique was applied to a mixture of N_2 and UF_6. Figure 10 shows the results of these experiments. The inverse lifetime of an excited N_2 molecular state is plotted versus the total pressure (UF_6 + N_2 partial pressure). As can be seen in Figure 10, for pure N_2 the inverse lifetime is linearly related to the pressure. The lifetime of a state is determined by depopulation by collisions. The collision time is

$$t = \frac{\lambda}{\bar{v}} \qquad \lambda \text{ : mean free path} \quad \bar{v} \text{ : average velocity}$$

since λ is related to the cross section σ by

$$\lambda = \frac{1}{n\sigma} \qquad n \text{ : particle density}$$

and the pressure is related to n by

$$p = nkT$$

assuming that

$$\bar{v} = \sqrt{\frac{8kT}{\pi m}}$$

$$\frac{1}{t} = p\sigma\sqrt{\frac{8}{\pi mkT}} \; .$$

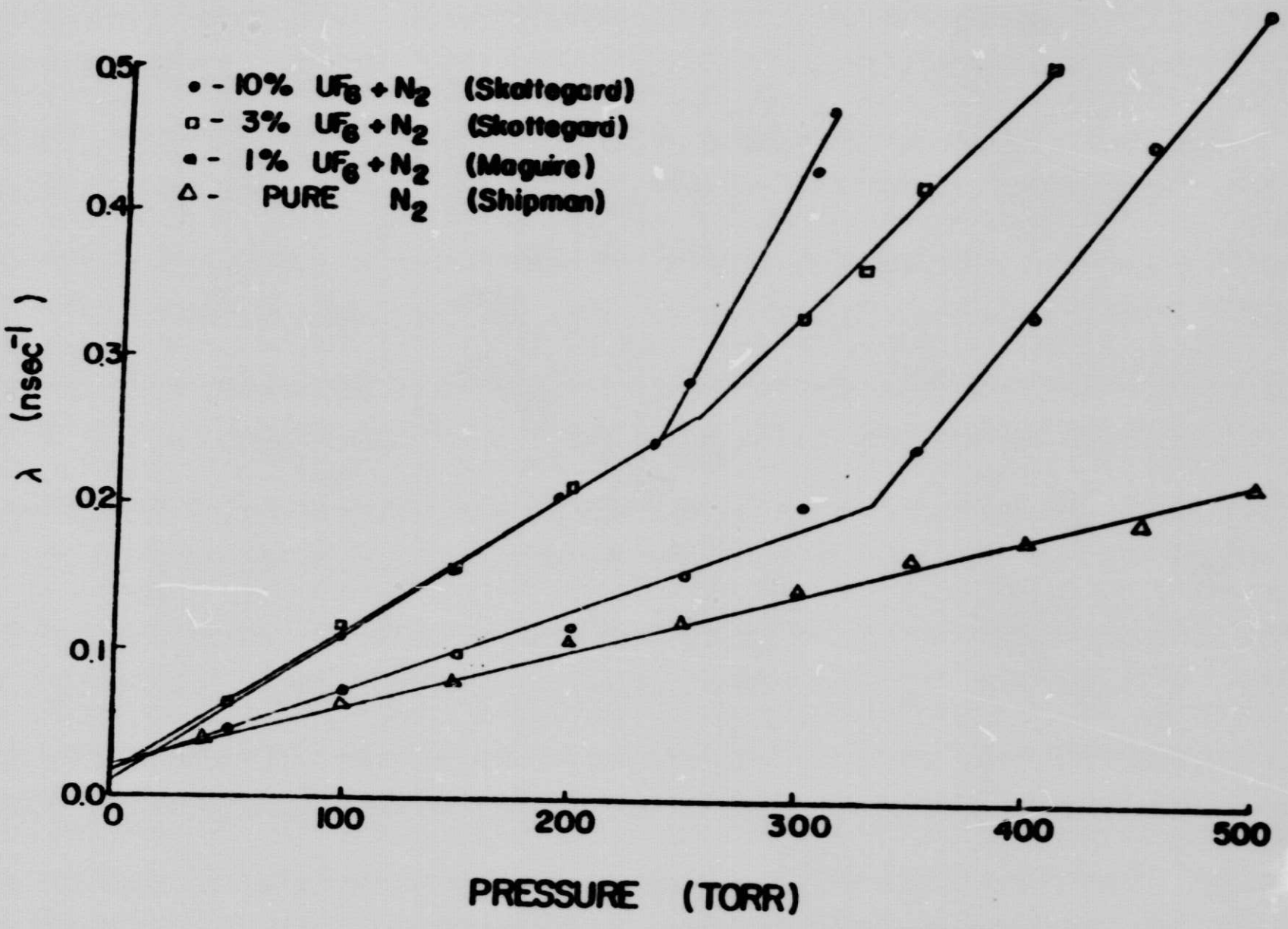

FIG. 10. Inverse Lifetime of N_2 versus Pressure

For this reason, the inverse lifetime should be, indeed, linearly related to the pressure. Only if the cross-section σ is also a function of pressure, could a nonlinear relationship be expected.

If UF_6 is added to the nitrogen gas, a shorter lifetime for the excited N_2 states is measured or, in other words, quenching of N_2 by UF_6 results. In Figure 10 a still linear relationship is observed, only the slope of the straight line is different. In the above equation, the absolute value of σ would have to be changed, which is reasonable since now collisions between UF_6 and N_2 are added into the picture. However, what is harder to explain is the apparent threshold for this larger cross section.

Since nuclear pumped lasers need to be high power and efficient, other systems such as excimer lasers need to be examined. The next gas studied therefore was XeF. By mixing Xe with a florine doner such as NF_3 the XeF molecule can be produced. With the addition of Ne as a buffer gas such studies have been done which parallel mixtures of functioning lasers.

Figure 11 shows a typical lifetime measurement for XeF, while Figure 12 gives a comparison of the measurements taken at total pressures of 300, 500, 700 and 900 torr. By measuring the slope of the exponential the lifetime can be found. The plot of 1/τ (Figure 12) shows these lifetimes as a function of pressure. Additional UF_6 changed the lifetime considerably. Figure 13 is a plot of the data with only 1% UF_6 added. It is obvious that the lifetime is shortened by addition of just a small percentage of UF_6.

REPRODUCIBILITY OF THE
ORIGINAL PAGE IS POOR

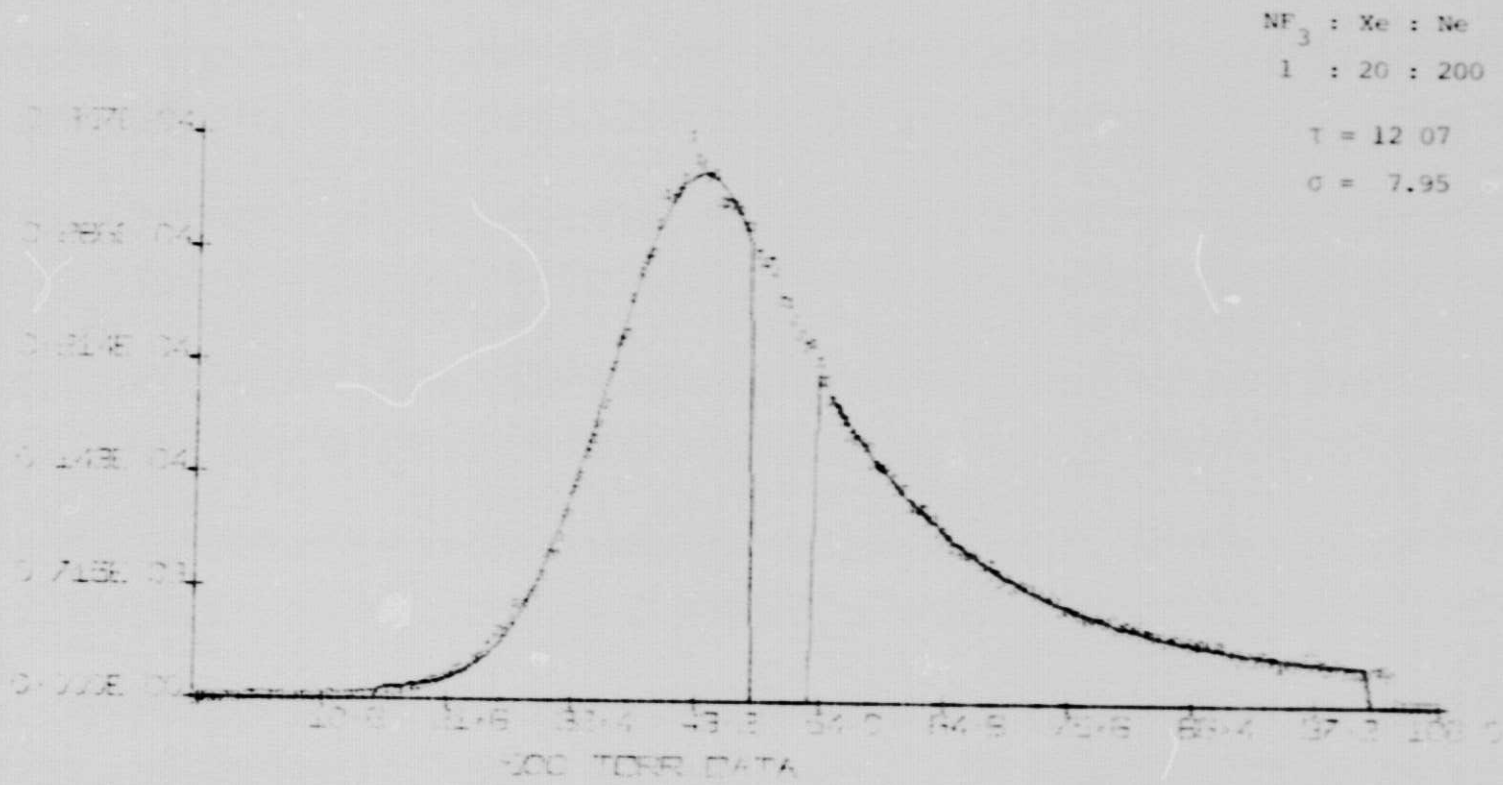

FIG. 11. Printout of Lifetime Measurements

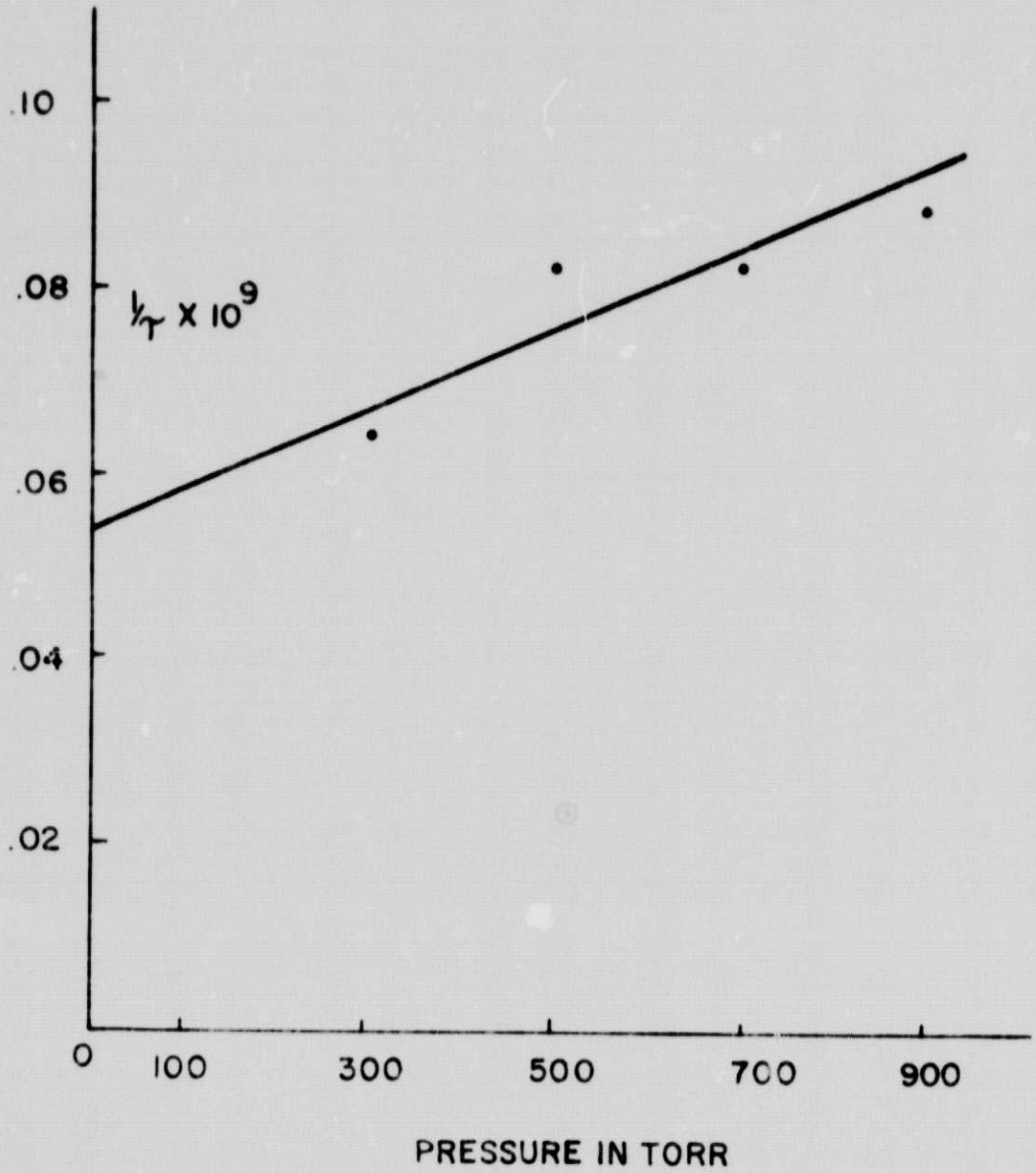

FIG. 12. LIFETIME OF XeF VERSUS PRESSURE

REPRODUCIBILITY OF THE
ORIGINAL PAGE IS POOR

REPRODUCIBILITY OF THE
ORIGINAL PAGE IS POOR

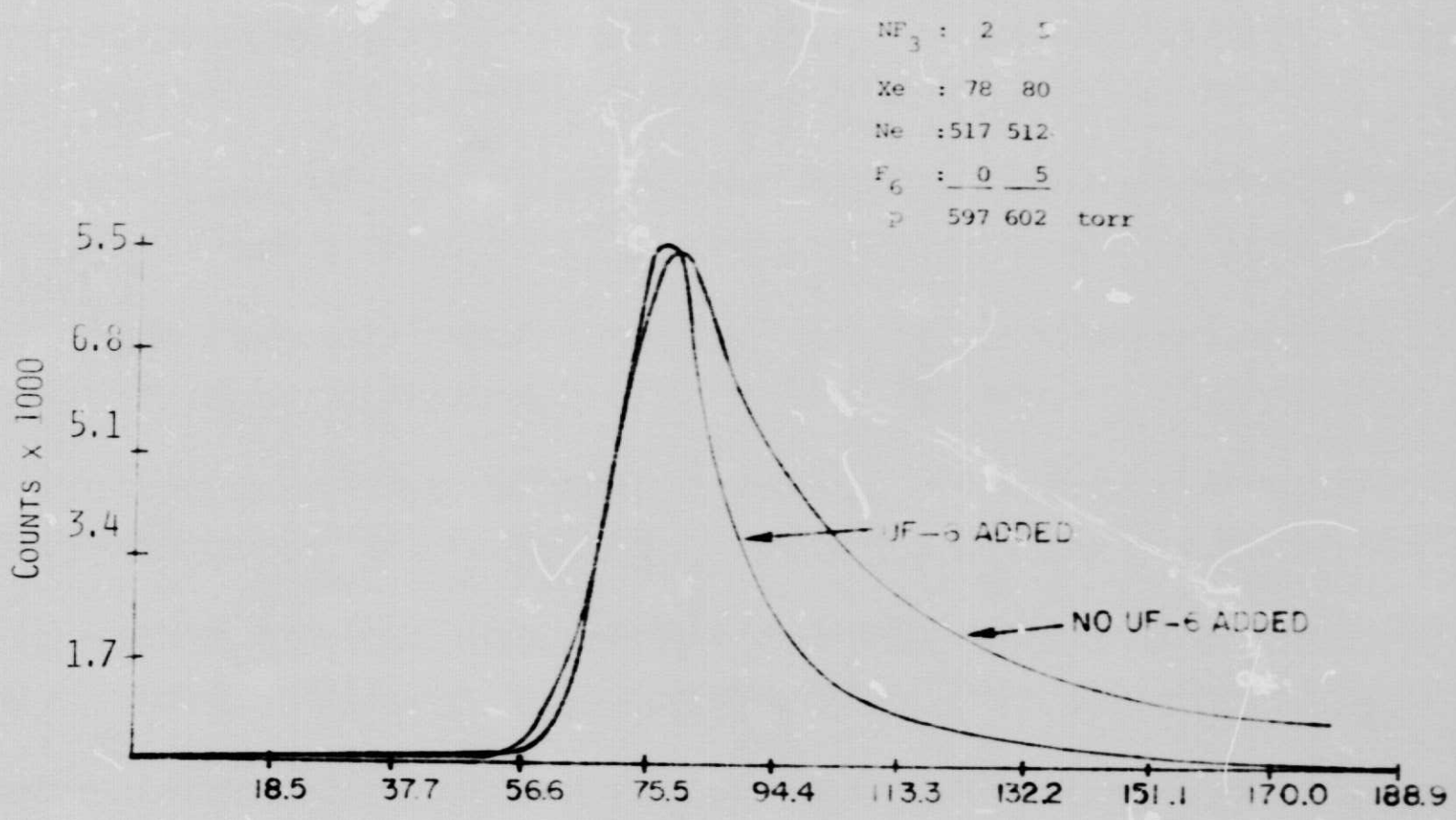

FIG. 13. Comparison of XeF Lifetime With and Without UF_6

APPENDIX

NUCLEAR-PUMPED CW-LASING OF THE ^{3}He-Ne SYSTEM

by

B.D. Carter, M.J. Rowe, R.T. Schneider
Department of Nuclear Engineering Sciences
University of Florida
Gainesville, Florida 32611

Submitted to Applied Physics Letters

August, 1979

NUCLEAR-PUMPED CW-LASING OF THE ^{3}He-Ne SYSTEM

by

B.D. Carter, M.J. Rowe, R.T. Schneider
Department of Nuclear Engineering Sciences
University of Florida
Gainesville, Florida 32611

ABSTRACT

The gain for the 6328Å laser line for the nuclear excited He-Ne system has been measured for 300 torr pressure at thermal neutron flux levels from 2×10^7 to 1×10^{14} n/cm^2-sec. In order to estimate small signal gain, the gain was also measured as a function of input intensity. For demonstration of feasibility of CW-operation of nuclear pumped lasers, a cavity was operated and lasing was observed. Although the laser output was small, we conclude that lasing in a CW mode has been achieved with He-Ne using moderate neutron flux levels.

INTRODUCTION

To show the feasibility of extracting power from a nuclear reactor in the form of laser light, it is mandatory to demonstrate that CW-laser action is possible. So far, the nuclear pumped lasers that have been demonstrated used pulsed reactors having extremely high neutron fluxes as energy sources.[1,2,3] Pulse lengths varied with the different experiments but, in all cases, were a small fraction of a second. For engineering applications of these lasers, a pulsed reactor with a high repetition rate would be required. Such reactors do not exist at present, although it is conceivable that they could be developed. However, it would be much easier if a steady state reactor, having a moderate neutron flux, could be used. This paper described the work done culminating in the actual CW nuclear pumped lasing of the He-Ne system.

GAIN MEASUREMENTS

Single pass gain experiments were carried out in two different reactors. The first, a medium flux tank type heavy-water reactor, located at the Georgia Institute of Technology, was used for the thermal neutron flux range from 1×10^{9} to 1×10^{14} n/cm^{2}-sec. The other reactor, an Argonaut type reactor located at the University of Florida, was used for lower thermal neutron fluxes ranging from 2×10^{4} to 2×10^{12} n/cm^{2}-sec. The overlap in ranges allowed comparison of the data taken at each reactor.

A. Medium Flux Reactor Gain Measurements

Figure 1 shows the experimental arrangement typical of both reactors. However, in the medium flux reactor, it is possible to irradiate larger volumes with a constant flux. Also, the access port is 6 inches in diameter as compared with 1.6 inches in the low flux facility. An He-Ne amplifier

REPRODUCIBILITY OF THE
ORIGINAL PAGE IS POOR

was located in a throughport close to the reactor core. The amplifier consisted of a water-cooled stainless-steel tube, terminated by two sapphire windows. It was filled with a ^{3}He-Ne (5:1) mixture of a total pressure of 300 Torr. At the entrance of the throughport a commercially available .5mW He-Ne oscillator was located. The amplified laser beam was projected onto the entrance slit of a monochromator and detected by a photomultiplier tube. The resulting photocurrent was measured with a picoammeter and continuously displayed on an x-y plotter. In the throughport, a maximum neutron density of 1×10^{14} was available for the ^{3}He(n,p)T reaction to excite the laser gas.

Figure 2 shows the results of the gain measurement. A peak power gain of 8.84 dB/m for the neon $^3s_2 - {}^2p_4$ laser transition (λ = 6323.2Å) was observed. This maximum amplification was achieved at a neutron flux of 2×10^{12} n/cm^2-s. At higher neutron fluxes, the gain decreased and turned into absorption. This agrees with the electrically pumped case where at large discharge tube currents, the output falls off and eventually ceases due to overdriving the laser medium. This overdriving is a result of destruction of the He 2's metastables by collisions of the second kind with electrons.[4] These measurements can be compared to older results which concerned nuclear enhancement of an electrically excited pulsed He-Ne laser.[5] The fact that their laser was electrically excited and operated at a lower gas pressure makes comparison difficult; however, the reason why no large gain was observed in this older work can be found in the fact that they were made at a neutron flux of $n \approx 10^{15}$ n/cm-sec, where, according to the present measurements, no gain can be expected.[5]

The power deposition in the laser amplifier was ~12 mW/cm^3 at peak gain, while ~4×10^{-3} mW/cm^3 was extracted in the form of laser light. This results in an efficiency of about 0.04%.

REPRODUCIBILITY OF THE
ORIGINAL PAGE IS P

B. Low Flux Reactor Gain Measurements

The first experiment indicated that the University of Florida training reactor, a low flux reactor (max 2×10^{12} n/cm^{2}sec) would be sufficient to continue the study of He-Ne.

A stainless steel capsule similar to that used previously, but uncooled, was inserted into the horizontal throughport of the reactor, see Figure 1. A commercial helium neon laser was used for the gain measurements. A beam splitter and a filter holder were inserted into the optical path.

The beam splitter, used in conjunction with a pyroelectric detector, allowed checking of constancy of the input beam. The filter holder provided a means to insert various filters into the light beam. Therefore, it was possible to measure gain for various input intensities.

On the output side of the amplifier cell a series of mirrors were used to project the beam onto the slit of a one meter spectrometer turned to the first order 6328Å laser wavelength, which ensured that only the 6328Å laser light would be detected by the photomultiplier tube. The photomultiplier output was amplified and fed into one channel (A) of a differential amplifier while the output of the pyroelectric detector was fed into the other channel (B) of this differential amplifier, to eliminate the possibility of variations in the output of the probe laser being mistaken for gain.

The probe laser used provided the opportunity for a second measurement technique independent of the differential amplifier. The laser had a high frequency noise component in its output. This component was also amplified in the gain cell. By measuring this noise component, one can calculate gain in the same way as the AC gain is found in a transistor circuit.

The results of these measurements can be seen in Figure 2.

REPRODUCIBILITY OF THE
ORIGINAL PAGE IS POOR

B. Low Flux Reactor Gain Measurements

The first experiment indicated that the University of Florida training reactor, a low flux reactor (max 2×10^{12} n/cm^{2}sec) would be sufficient to continue the study of He-Ne.

A stainless steel capsule similar to that used previously, but uncooled, was inserted into the horizontal throughport of the reactor, see Figure 1. A commercial helium neon laser was used for the gain measurements. A beam splitter and a filter holder were inserted into the optical path.

The beam splitter, used in conjunction with a pyroelectric detector, allowed checking of constancy of the input beam. The filter holder provided a means to insert various filters into the light beam. Therefore, it was possible to measure gain for various input intensities.

On the output side of the amplifier cell a series of mirrors were used to project the beam onto the slit of a one meter spectrometer turned to the first order 6328Å laser wavelength, which ensured that only the 6328Å laser light would be detected by the photomultiplier tube. The photomultiplier output was amplified and fed into one channel (A) of a differential amplifier while the output of the pyroelectric detector was fed into the other channel (B) of this differential amplifier, to eliminate the possibility of variations in the output of the probe laser being mistaken for gain.

The probe laser used provided the opportunity for a second measurement technique independent of the differential amplifier. The laser had a high frequency noise component in its output. This component was also amplified in the gain cell. By measuring this noise component, one can calculate gain in the same way as the AC gain is found in a transistor circuit.

The results of these measurements can be seen in Figure 2.

REPRODUCIBILITY OF THE
ORIGINAL PAGE IS POOR

These measurements agreed within reason with the preliminary measurements made at the medium flux reactor. In addition, these measurements are now extended to lower flux levels.

Differences between the measurements done at the two different locations pertain to the neutron flux range between 10^{11} n/cm^{2}sec and 10^{13} n/cm^{2}sec. The uncooled laser tube shows a maximum gain at 6×10^{11} n/cm^{2}sec while the cooler laser tube shows the maximum gain at 1×10^{12} n/cm^{2}sec. Since both measurements tend to agree at the lower flux levels, it is suggested that the gain curves at higher fluxes are due to the fact that the uncooled tube is heated by the nuclear reactions which is detrimental to laser performance. It was found that when the capsule was cool (start of the run) gain was found, but after running the reactor at power for a few minutes, thus heating the amplifier, gain disappeared. Then, when the capsule was allowed to cool and gain measurements repeated, gain was again found.

The reason that an attempt was made at all to use an uncooled tube is that the access port for the low flux reactor is only 1.6" in diameter, while the one for the medium flux reactor was 6" in diameter. It is difficult to reduce the complete instrument package to the smaller diameter. On the other hand, this reactor offers operational characteristics, which are better for the neutron flux range of interest than the one of the medium flux reactor which is designed to operate at 10^{13} n/cm^{2}sec, and higher.

In order to assure that small signal gain can be determined, it is necessary to measure gain for different input intensities. This was done with reactor power as parameter. Due to the heating effect, the reactor power was restricted to the region between 5 and 30 KW where heating does not produce a marked increase in the tube temperature.

The results of these measurements are shown in Figure 3. As can be seen, the gain measured for small signals is, indeed, substantial (up to

REPRODUCIBILITY OF THE
ORIGINAL PAGE IS POOR

800%), however, as a consequence, saturation is reached at fairly low input levels as well. Therefore, only low power laser output can be expected for a nuclear pumped HeNe laser, which is in agreement with the situation of the discharge He-Ne Laser.

LASER EXPERIMENT

To demonstrate lasing for a He-Ne nuclear pumped laser, the experiment as shown in Figure 1b was set up.

The laser cavity designed to resonate at 6328Å, used a corner cube reflector and a 20 m-radius, dielectric output mirror.

The corner cube reflector was used in order to reduce the alignment problems for incore reactor experimentation. It was felt that due to the extremely high single pass gain, a corner cube reflector, instead of a regular laser mirror, could be tolerated. Although the cavity had single pass losses of 51%, the single pass gain measurements indicated this cavity would be sufficient to support lasing.

This proved, indeed, to be the case and Figure 4 shows the laser output as a function of neutron flux. Due to the inability to calibrate the detection system for absolute units, only relative output is plotted. Although based on the sensitivity of the photomultiplier tube at 6328Å, it's peak output was estimated to be a few microwatts.

The threshold for lasing is at a neutron flux level of 2×10^{11} n/cm^2-sec. After threshold, the plot of laser output follows the increase in neutron flux. After a short time at full reactor power, lasing ceased due to the heating of the capsule as predicted in the gain measurements.

REPRODUCIBILITY OF THE
ORIGINAL PAGE IS POOR

CHECKS FOR LASING

First, a wavelength scan with the spectrometer was performed to insure that the observed phenomenon is, indeed, a spectrum line and not a cutout of a continuum. Optical materials, like sapphire, which are used as window material in the present tube, luminesce under influence of nuclear radiation.[6] This radiation output is also proportional to reactor power and could product a similar plot as Figure 4. However, the sapphire luminescence peaks at blue wavelengths and is continuous radiation. Detection of a red line would discard the possibility that sapphire light was observed. The wavelength scan showed several red lines, the strongest being at 6328Å.

Next, the resonant cavity was spoiled and the wavelength scan repeated Under these conditions, only spontaneous light output can be expected. The ratio of spontaneous to stimulated output was found to be $\frac{I_{stim}}{I_{spon}} \approx 60$. There is substantial error in the measurements attached to this value because, like most laser lines, the 6328Å is a weak spectrum line resulting in a low spontaneous intensity. However, the error is less than a factor of 60 and there is, undoubtedly, a laser output.

REFERENCES

1. H. H. Helmick, J. L. Fuller, and R. T. Schneider, "Direct Nuclear Pumping of a Helium Xenon Laser," Appl. Phys. Lett., 26, 6, 327 (1975).
2. R. J. DeYoung, N. W. Jalufka, F. Hohl and M. D. Williams, "Direct Nuclear Pumped Lasers Using Volumetric He^3 Reaction," Proceedings of the Princeton University Conference on Partially Ionized Plasmas Including the Third Symposium on Uranium Plasmas, (1976).
3. Proceedings from the First International Symposium on Fission Induced Plasmas and Nuclear Pumped Lasers, (May 23-24, 1978), Paris, France.
4. A. E. Siegman, An Introduction to Lasers and Masers. New York: McGraw-Hill Book Company, 1971.
5. J. C. Guyot, G. H. Miley, J. T. Verdeyen, and T. Ganely, "On Gas Laser Pumping via Nuclear Radiation," Trans. Symp. Research on Uranium Plasmas and Their Technological Applications, NASA SP-236, (1970).
6. R. N. Davie, J. F. Davis, and R. T. Schneider, "Observations on the Luminescence of α-Al_2O_3 (Synthetic Sapphire) in the Reactor Environment," Nuclear Technology, 31, 276-278, (1976).

TABLE OF FIGURES

Figure 1: Experimental Set-up

Figure 2: Gain vs. Neutron Flux for Cooled and Uncooled Amplifier

Figure 3: Determination of Small Signal Gain

Figure 4: Laser Output as a Function of Neutron Flux

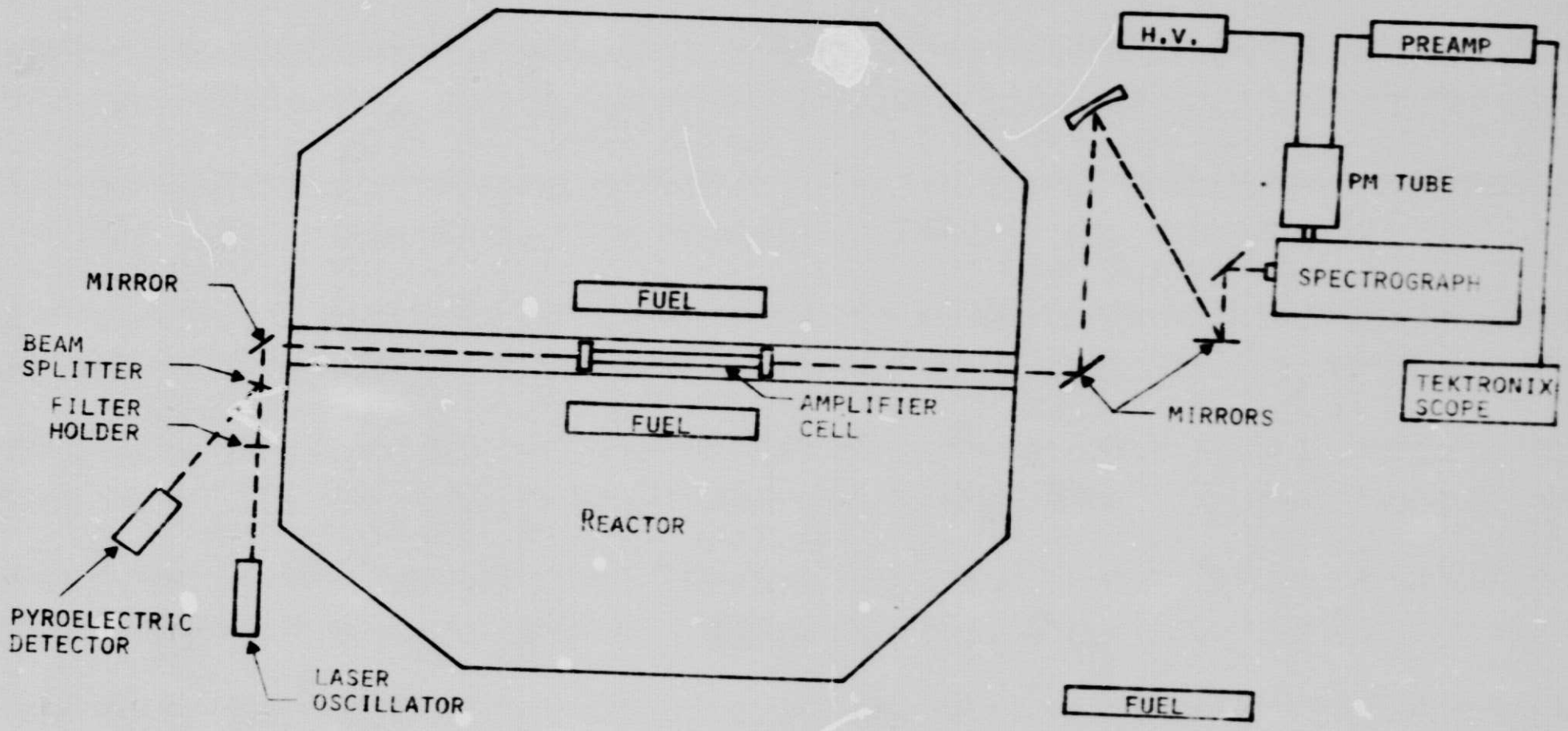

A. AMPLIFIER ARRANGMENT

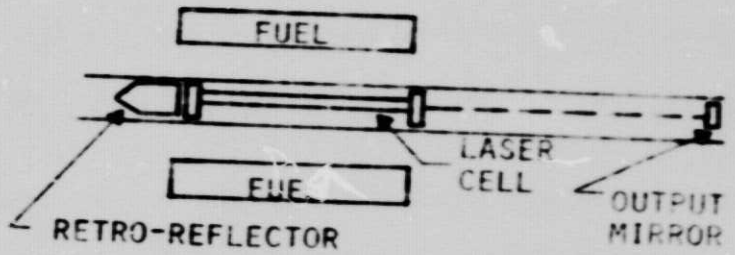

B. CAVITY TO DEMONSTRATE LASER ACTION

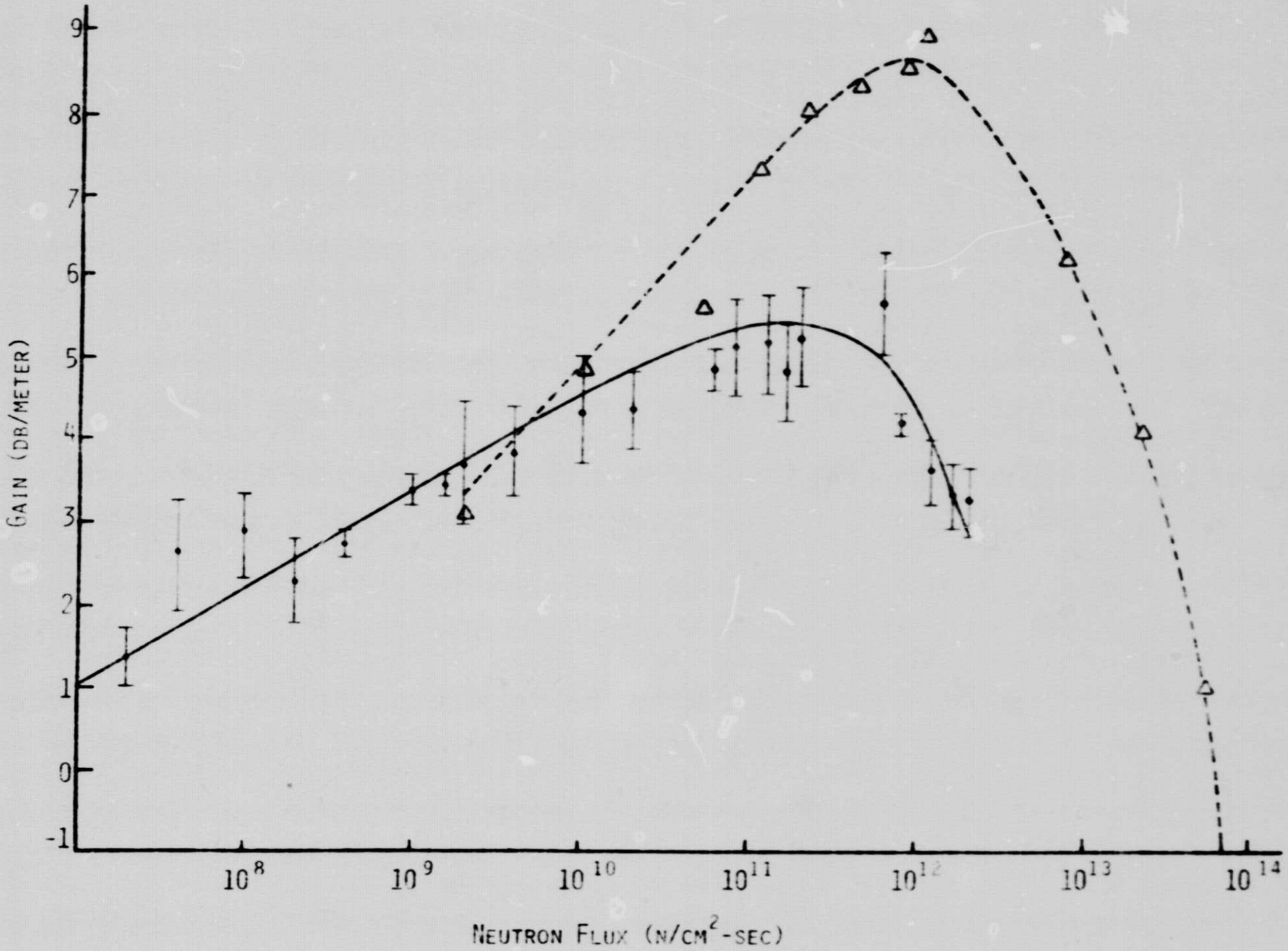
GAIN (DB/METER)
9
8
7
6
5
4
3
2
1
0
-1
10^8
10^9
10^{10}
10^{11}
10^{12}
10^{13}
10^{14}
NEUTRON FLUX (N/CM^2-SEC)

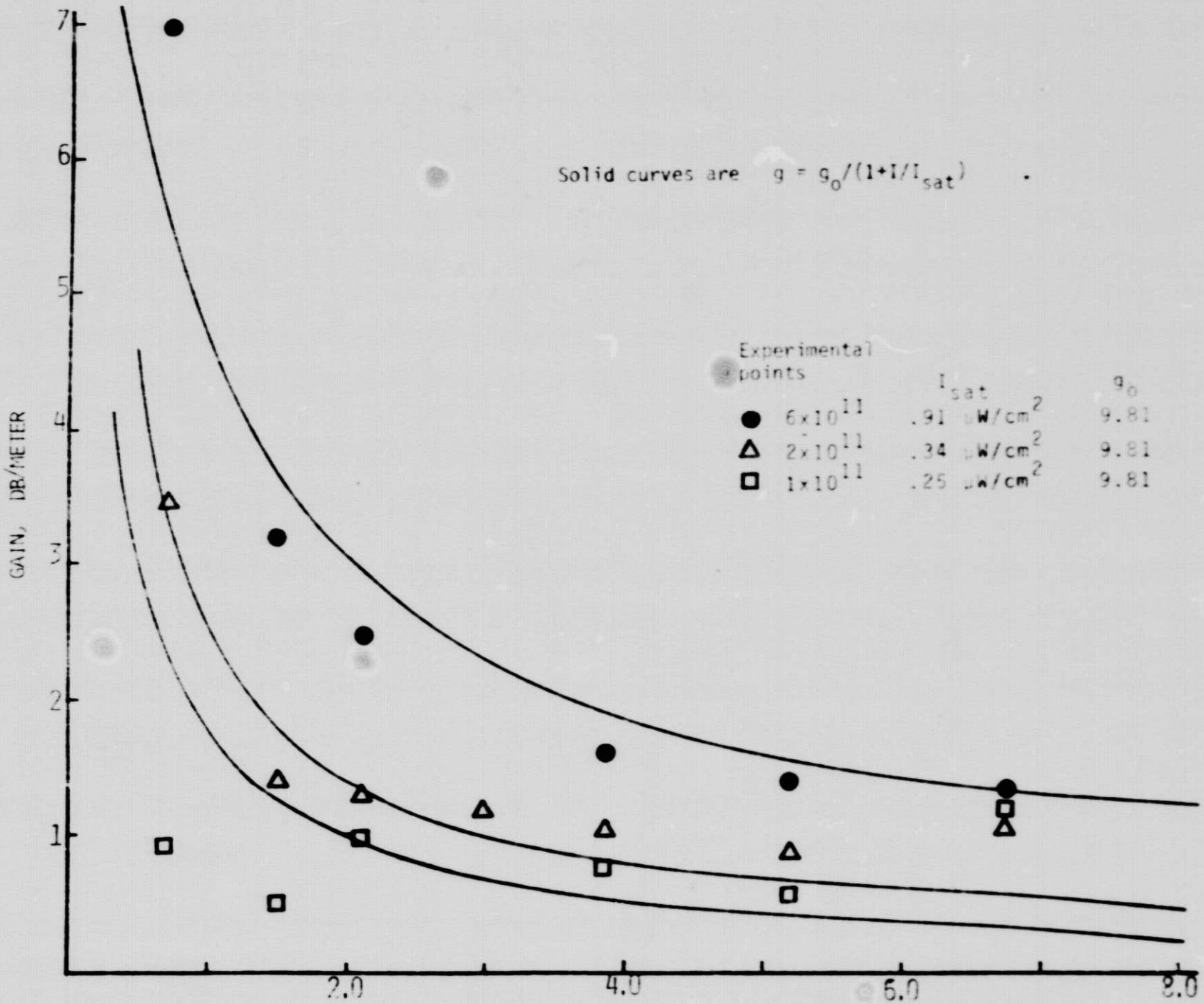
Solid curves are $g = g_o/(1+I/I_{sat})$.
Experimental points
I_{sat}
g_o
6×10^{11} .91 μW/cm^2 9.81
2×10^{11} .34 μW/cm^2 9.81
1×10^{11} .25 μW/cm^2 9.81
GAIN, DB/METER
7
6
5
4
3
2
1
2.0
4.0
6.0
8.0

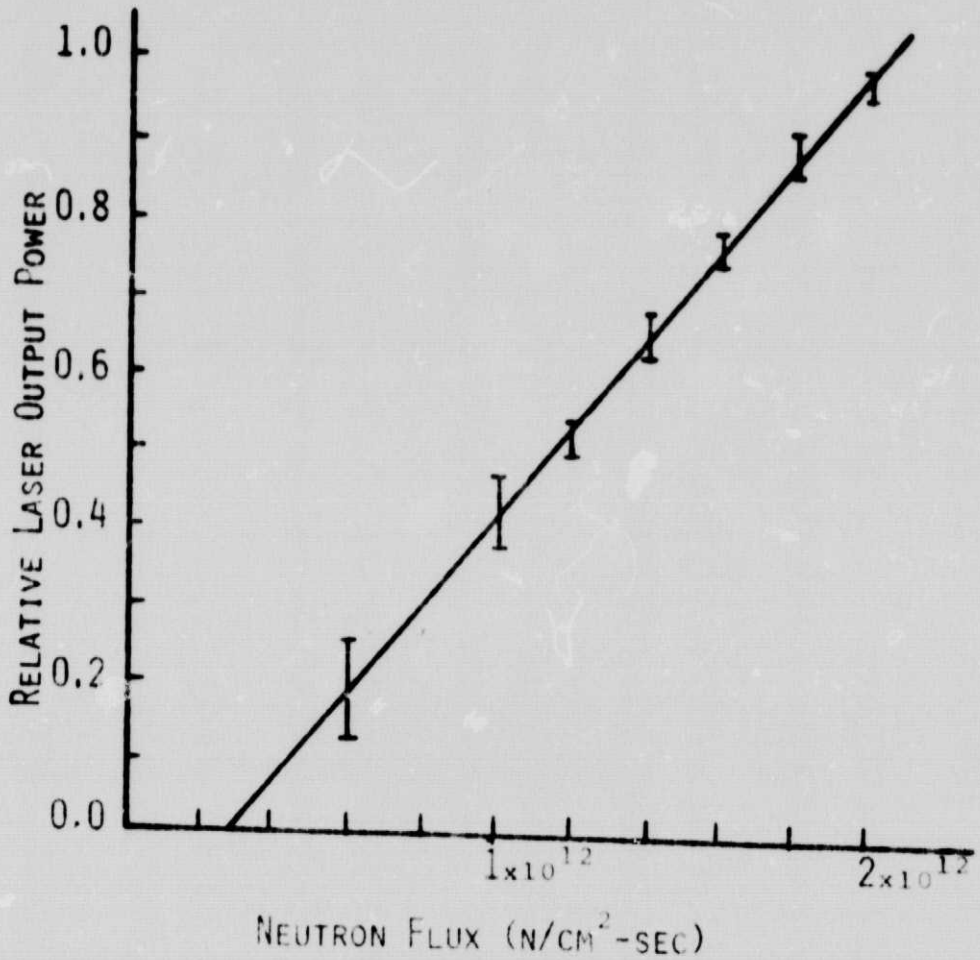
1.0
0.8
0.6
0.4
0.2
0.0
Relative Laser Output Power
1x10^12
2x10^12
Neutron Flux (N/cm^2-sec)

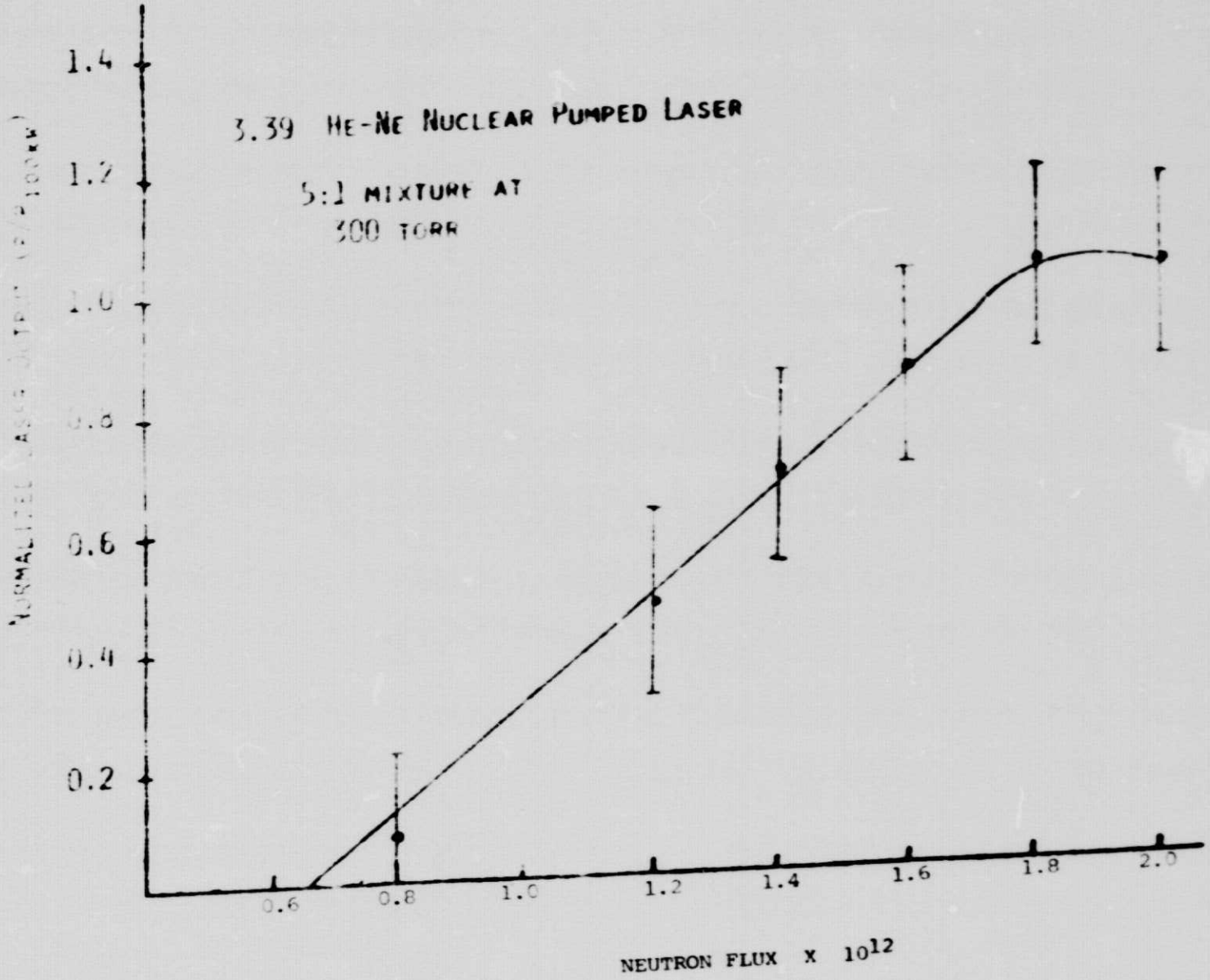
3.39 HE-NE NUCLEAR PUMPED LASER
5:1 MIXTURE AT
300 TORR
1.4
1.2
1.0
0.8
0.6
0.4
0.2
0.6
0.8
1.0
1.2
1.4
1.6
1.8
2.0
NEUTRON FLUX X 10^{12}